European Radiology
EUROPEAN SOCIETY OF RADIOLOGY

IMAGING INFORMATICS AND ARTIFICIAL INTELLIGENCE

Late gadolinium enhanced cardiac MR derived radiomics approach for predicting all-cause mortality in cardiac amyloidosis: a multicenter study

Xi Yang Zhou[1,2] · Chun Xiang Tang[2] · Ying Kun Guo[3] · Wen Cui Chen[4] · Jin Zhou Guo[4] · Gui Sheng Ren[4] · Xiao Li[5] · Jun Hao Li[1,2] · Guang Ming Lu[2] · Xiang Hua Huang[4] · Yi Ning Wang[5] · Long Jiang Zhang[2] · Gui Fen Yang[1]

Abstract

Objectives To evaluate the prognostic value of radiomics features based on late gadolinium enhancement (LGE) cardiac magnetic resonance (CMR) images in patients with cardiac amyloidosis (CA).

Methods This retrospective study included 120 CA patients undergoing CMR at three institutions. Radiomics features were extracted from global and three different segments (base, mid-ventricular, and apex) of left ventricular (LV) on short-axis LGE images. Primary endpoint was all-cause mortality. The predictive performance of the radiomics features and semi-quantitative and quantitative LGE parameters were compared by ROC. The AUC was used to observe whether Rad-score had an incremental value for clinical stage. The Kaplan–Meier curve was used to further stratify the risk of CA patients.

Results During a median follow-up of 12.9 months, 30% (40/120) patients died. There was no significant difference in the predictive performance of the radiomics model in different LV sections in the validation set (AUCs of the global, basal, middle, and apical radiomics model were 0.75, 0.77, 0.76, and 0.77, respectively; all $p > 0.05$). The predictive performance of the Rad-score of the base-LV was better than that of the LGE total enhancement mass (AUC:0.77 vs. 0.54, $p < 0.001$) and LGE extent (AUC: 0.77 vs. 0.53, $p = 0.004$). Rad-score combined with Mayo stage had better predictive performance than Mayo stage alone (AUC: 0.86 vs. 0.81, $p = 0.03$). Rad-score (≥ 0.66) contributed to the risk stratification of all-cause mortality in CA.

Conclusions Compared to quantitative LGE parameters, radiomics can better predict all-cause mortality in CA, while the combination of radiomics and Mayo stage could provide higher predictive accuracy.

Clinical relevance statement Radiomics analysis provides incremental value and improved risk stratification for all-cause mortality in patients with cardiac amyloidosis.

Key Points

● *Radiomics in LV-base was superior to LGE semi-quantitative and quantitative parameters for predicting all-cause mortality in CA.*
● *Rad-score combined with Mayo stage had better predictive performance than Mayo stage alone or radiomics alone.*
● *Rad-score ≥ 0.66 was associated with a significantly increased risk of all-cause mortality in CA patients.*

Drs. Zhou and Tang had equal contribution to this work.

✉ Long Jiang Zhang
 kevinzhlj@163.com

✉ Gui Fen Yang
 ygfnstl@163.com

1 Department of Nuclear Medicine, Jinling Hospital, Medical School of Nanjing University, Nanjing 210002, Jiangsu, China

2 Department of Radiology, Jinling Hospital, Medical School of Nanjing University, Nanjing 210002, Jiangsu, China

3 Department of Radiology, West China Second University Hospital, Sichuan University, 20# South Renmin Road, Chengdu 610041, Sichuan, China

4 National Clinical Research Center of Kidney Disease, Jinling Hospital, Nanjing University School of Medicine, Nanjing 210002, Jiangsu, China

5 Department of Radiology, Peking Union Medical College Hospital, Chinese Academy of Medical Sciences & Peking Union Medical College, No. 1, Shuaifuyuan, Dongcheng District, Beijing 100730, China

Abbreviations

AL	Immunoglobulin light chain
CA	Cardiac amyloidosis
CMR	Cardiac magnetic resonance
cTNT	Cardiac troponin T
EF	Ejection fraction
FA	Flip angle
ICC	Intra-class correlation coefficient
LGE	Late gadolinium enhancement
LV	Left ventricular
NT-proBNP	N-terminal pro B-type natriuretic peptide
PSIR	Phase-sensitive reconstruction
Rad-score	Radiomics score
RV	Right ventricular
SD	Standard deviation
SSFP	Steady-state free precession
TE	Echo time
TR	Repetition time

Introduction

Cardiac amyloidosis (CA) is caused by the accumulation of amyloid fibrils in cardiac tissue, which induces diastolic dysfunction [1–3]. Immunoglobulin light chain (AL) amyloidosis is the most common type of CA [4]. Up to 50% of patients with AL amyloidosis have cardiac involvement, which is the leading cause of morbidity and mortality in these patients [5–7]. If untreated, the median survival time is less than 6 months [2, 8]. Therefore, timely monitoring of indicators related to the prognosis of CA is essential for prognostic improvement of CA patients.

Clinically, Mayo stage based on N-terminal pro B-type natriuretic peptide (NT-proBNP, ≥ 1800 pg/mL) and cardiac troponin T (cTNT, ≥ 0.025 ng/mL) and difference in serum-free light chains (≥ 18 mg/dL) has been prognostically validated for risk stratification of CA patients [9, 10]. However, these serum biomarkers lack specificity and are influenced by renal impairment [6]. Thus, to explore other prognostic indicators of CA becomes an important task. With the rapid development of cardiac magnetic resonance (CMR) technology, the prognostic indicators of CA have increased, significantly improving the prediction power of adverse events in CA. CMR is an accurate and highly reproducible measurement that offers comprehensive cardiac structure and function evaluation as well as myocardial tissue characterization [11]. CMR with the late gadolinium enhancement (LGE) technique is considered the imaging modality of choice for the identification of CA with high diagnostic and prognostic value [12–14]. However, because the identification of LGE is based on the difference between abnormal and normal tissues, it may underestimate the extent of disease progression when lesions are not significantly enhanced in early stages

or are diffusely enhanced in late stages, thus affecting the assessment of prognosis [11].

Since LGE is closely related to clinical, morphological, and functional markers [14], there is an urgent need to mine more prognostic information from LGE images. Radiomics can reveal vital information invisible to the human eye by extracting quantitative information from imaging data [15–17]. Previous studies [18–20] have reported the potential of CMR radiomics in predicting important clinical outcomes in cardiovascular disease, such as providing incremental information about adverse cardiac events in patients with myocardial infarction [21]. However, no prognostic role of radiomics in CA has been explored. We hypothesize that radiomics analysis will abstract important invisible information of LGE to predict the future outcome of CA patients. Therefore, the aim of this exploratory study was to extract radiomics features of LGE-CMR images of CA patients in order to assess their potential prognostic performance and further risk stratify patients.

Methods

Patients

We collected 200 patients with AL amyloidosis undergoing CMR between 2012 and 2020 from 3 tertiary medical centers of three different regions of China. All patients had histological evidence of systemic AL amyloidosis based on positive Congo red stain and light chain deposition. ATTR form of the disease was not included. Only patients with myocardial involvement were included in this study, while patients without myocardial involvement were excluded. CA was managed and diagnosed based on the current guidelines [22, 23]. Cardiac involvement was confirmed according to positive extracardiac biopsy accompanied either by echocardiography evidence of left ventricular (LV) wall thickening ≥ 12 mm in the absence of any other known causes, or NT-proBNP > 332 ng/L in the absence of renal insufficiency and atrial fibrillation. Severity of CA was classified into four stages according to the revised Mayo stage published in 2012 [9]. The Mayo stage details and Mayo stage of each patient in different centers and different groups are shown in Supplemental Appendix, Supplemental Table 1, and Table 1.

CMR acquisition and LGE analysis

The details of CMR scanners and sequence are provided in Supplemental Appendix. Myocardial enhancement was evaluated using a semi-quantitative score system (QALE) [24]. Each LV level is scored according to the degree of LGE. The range for each level in each patient is from 0 (no detectable LGE) to 4 (circumferential and transmural LV LGE), plus 6 if RV LGE is present [24, 25].

Table 1 Clinical characteristics, CMR parameters, and radiomics parameter in the CA patients

Variables	Total ($n = 120$)	Event-positive ($n = 40$)	Event-negative ($n = 80$)	p
Clinical parameters				
Male, n (%)	71 (59.2)	30 (75.0)	41 (51.2)	0.013
Age, years	56.1 ± 9.5	59.0 ± 10.4	54.6 ± 8.7	0.015
Cardiovascular risk factors, n (%)				
Hypertension	15 (12.5)	4 (10.0)	11 (13.8)	0.558
Hyperlipidemia	30 (25)	8 (20.0)	22 (27.5)	0.371
Diabetes mellitus	8 (6.7)	5 (12.5)	3 (3.8)	0.07
Coronary disease	1 (0.8)	0 (0.0)	1 (1.3)	0.478
Myocardial enzymes and stage				
Log cTNT (ng/mL)	− 1.3 ± 0.5	− 0.9 ± 0.4	− 1.5 ± 0.5	< 0.001
Log NT-pro-BNP	3.3 (2.7, 3.6)	3.7 ± 0.4	2.9 ± 0.6	< 0.001
Mayo (I/II/III/IV)	31/27/48/14	2/1/28/9	29/26/20/5	< 0.001
CMR parameters				
LVEF, %	57.6 (48.1, 67.3)	48.3 (38.6, 57.5)	61.6 (51.9, 70.4)	< 0.001
LVEDV, mL	107.0 (92.7, 131.4)	117.2 (95.1, 148.3)	103.1 (88.3, 125.2)	0.023
LVESV, (55.6,104.3)	45.1 (29.9, 61.9)	56.9 (46.5, 83,2)	37.9 (27.3, 49.3)	< 0.001
Myocardial volume, mL	72.9 (53.0, 99.6)	83.6 (61.0, 112.0)	66.63 (47.5, 96.6)	0.012
Myocardial mass, g	76.6 (55.6, 104.3)	87.6 (64.0, 115.4)	70.0 (49.9, 101.4)	0.016
Myocardial thickness, mm	14.53 ± 3.1	13.5 ± 2.6	16.6 ± 2.9	< 0.001
LGE total enhanced volume, mL	16.6 (5.0, 37.0)	20.8 (5.3, 36.5)	14.1 (4.5, 38.5)	0.538
LGE total enhanced mass, mL	17.4 (5.2, 38.9)	21.9 (5.5, 38.3)	14.8 (4.7, 40.4)	0.538
LGE extent, %	26.2 (8.4, 48.1)	26.9 (7.7, 37.4)	24.4 (8.4, 51.7)	0.624
Radiomics				
Rad-score (base)	0.43 (0.28, 0.64)	0.64 (0.44, 0.79)	0.39 (0.26, 0.49)	< 0.001

CA, cardiac amyloidosis; *cTNT*, cardiac troponin T; *NT-proBNP*, N-terminal pro B-type natriuretic peptide; *LGE*, late gadolinium enhancement; *Rad-score*, radiomics score

LV volumes, mass, ejection fraction (EF), and LGE extent were quantified using CVI 42 version 5.13.5 (Circle Cardiovascular Imaging lnc). For LGE quantification, a gray-scale threshold of 5 standard deviations (SD) above the mean signal intensity of myocardium was used [26]. Values of quantitative measurement of LGE were reported as a percentage of the LV enhanced area, the total enhanced mass, and the total enhanced volume.

Radiomics analysis

Segmentation

LGE segmentation, feature extraction, and model building were based on Dr. Wise Multimodal Research Platform (https://keyan.deepwise.com, V2.0).

Segmentation was performed on the base-to-apex slices of the short-axis LGE images by one cardiovascular radiologist (X.Y.Z. with 3 years of experience in CMR). For testing the reproducibility, image segmentation was repeated in 50 patients by another reader (J.H.L. with 3 years of experience in CMR) for interobserver analysis.

Feature extraction and dimension reduction

Radiomics features were extracted on the short-axis images for the entire LV, basal, middle, and apical portions, respectively. Image preprocessing and radiomics feature calculation methods are seen in Supplemental Appendix. To reduce the high dimensionality of the extracted texture features, the interobserver reproducibility was evaluated for all features using intra-class correlation coefficient (ICC), and those with high stability (ICC > 0.80) were kept for further analysis. To increase the robustness of the features, the included features were subjected to correlation analysis. When the linear correlation coefficient between any two independent variables on the training set was greater than 0.90, one of the features was removed to alleviate the redundancy between the features, making each feature independent of each other. Subsequently, the features correlated with the endpoint event were selected for further dimensionality reduction using a one-way analysis of variance feature screening method, and 5% of features with significant differences were retained. Logistic regression algorithm conducted by fivefold cross-validation was then
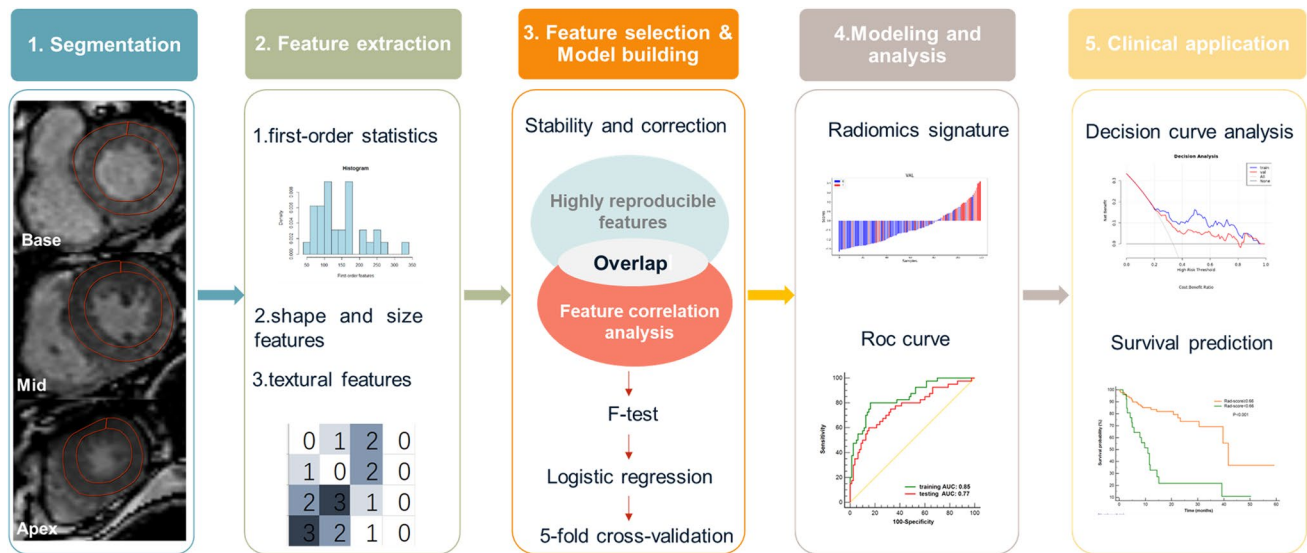
Fig. 1 The flow chart of LV segmentation and quantitative texture feature analysis

used to construct a radiomics signature. A radiomics signature was created by a linear combination of selected features weighted by their respective coefficients, and the corresponding radiomics score (Rad-score) was calculated for each patient. The radiomics workflow is shown in Fig. 1 and Supplemental Appendix.

Clinical outcomes

Follow-up of CA patients was completed independently in each center. All patients were followed up via clinic visit or telephone interview. The primary outcome was defined as all-cause mortality. Duration of follow-up was determined from the CMR study date to the occurrence of an endpoint or the date of the last clinical follow-up. Unless the outcome was death from any cause, patients were censored at the end of the study follow-up time. If patients were lost to follow-up, their last clinic visit record date was used.

Statistical analysis

Statistical analysis was performed using SPSS 26.0 (IBM Inc), MedCalc 19.6 (MedCalc Software Ltd), and X-tile 3.6.1(X-tile software). All continuous data were given as mean $\pm$ SD or median and 25–75th percentiles, while categorical data were presented as frequencies. NT-proBNP and troponin T were log transformed to achieve normality. Numerical variables were compared by means of the *t*-test or Mann–Whitney *U* test, and categorical variables were compared using the χ^2 test.

The performance of CMR parameters and radiomics in predicting endpoint events was evaluated using the area under the curve (AUC) and compared using the DeLong test. The optimal cut-point for continuous prognostic markers was obtained by using X-tile software to dichotomize feature. Survival curves for different Rad-score groups were depicted using the Kaplan–Meier method and compared using the log-rank test. The clinical utility of the model was evaluated with decision curve analysis. $p < 0.05$ was considered to indicate statistical significance.

Results

Patients

A total of 80 CA-negative patients were excluded, and 120 CA-positive patients (79 patients from Jinling Hospital, 19 patients from Peking Union Medical College Hospital, and 22 patients from the Second West China Hospital) were finally included. Forty endpoint events occurred during a median follow-up of 12.9 months (interquartile range 6.8, 22.4 months), including 1 sudden cardiac death, 1 heart failure, and 38 deaths of unknown cause. CA patients were divided into event-positive and event-negative groups according to the presence or absence of all-cause death. Patients in the event-positive group had higher levels of cTNT and NT-proBNP (all $p < 0.001$); thus, Mayo stage based on the above markers was also significantly higher. The two groups did not show statistically significant differences in the quantitative LGE parameters (total enhancement volume, total enhancement mass, and LGE extent). However, Rad-score in the event-positive group showed significantly higher at the base-LV than that of the event-negative group (0.64 vs.

Table 2 Predictive performance of radiomics models for different sections

Parameters	Global		Base		Midventricular		Apex	
	Training	Validation	Training	Validation	Training	Validation	Training	Validation
AUC	0.91	0.75	0.85	0.77	0.86	0.76	0.87	0.77
ACC	0.83	0.68	0.82	0.65	0.83	0.73	0.75	0.70
Sensitivity	0.90	0.75	0.70	0.60	0.68	0.48	0.87	0.75
Specificity	0.80	0.65	0.88	0.84	0.90	0.85	0.70	0.67
PPV	0.69	0.52	0.74	0.65	0.77	0.61	0.59	0.53
NPV	0.94	0.84	0.85	0.81	0.85	0.76	0.91	0.84

AUC, area under the curve; *ACC*, accuracy; *PPV*, positive predictive value; *NPV*, negative predictive value

0.39, $p < 0.001$). Other patients' characteristics and CMR parameters are reported in Table 1.

Radiomics features selection and construction

A total of 1906 radiomics features were extracted from the global, basal, middle, and apical segments of LGE images, respectively. After assessing the reproducibility and further dimensionality reduction, 16, 7, 9, and 22 radiomics features in the global, basal, middle, and apical sections were finally selected for model building. Logistic regression algorithm was used to rank the weight coefficients of the selected features and build the radiomics model. The weight coefficients of the 7 most relevant features at the base-LV selected from the training set included one original, one
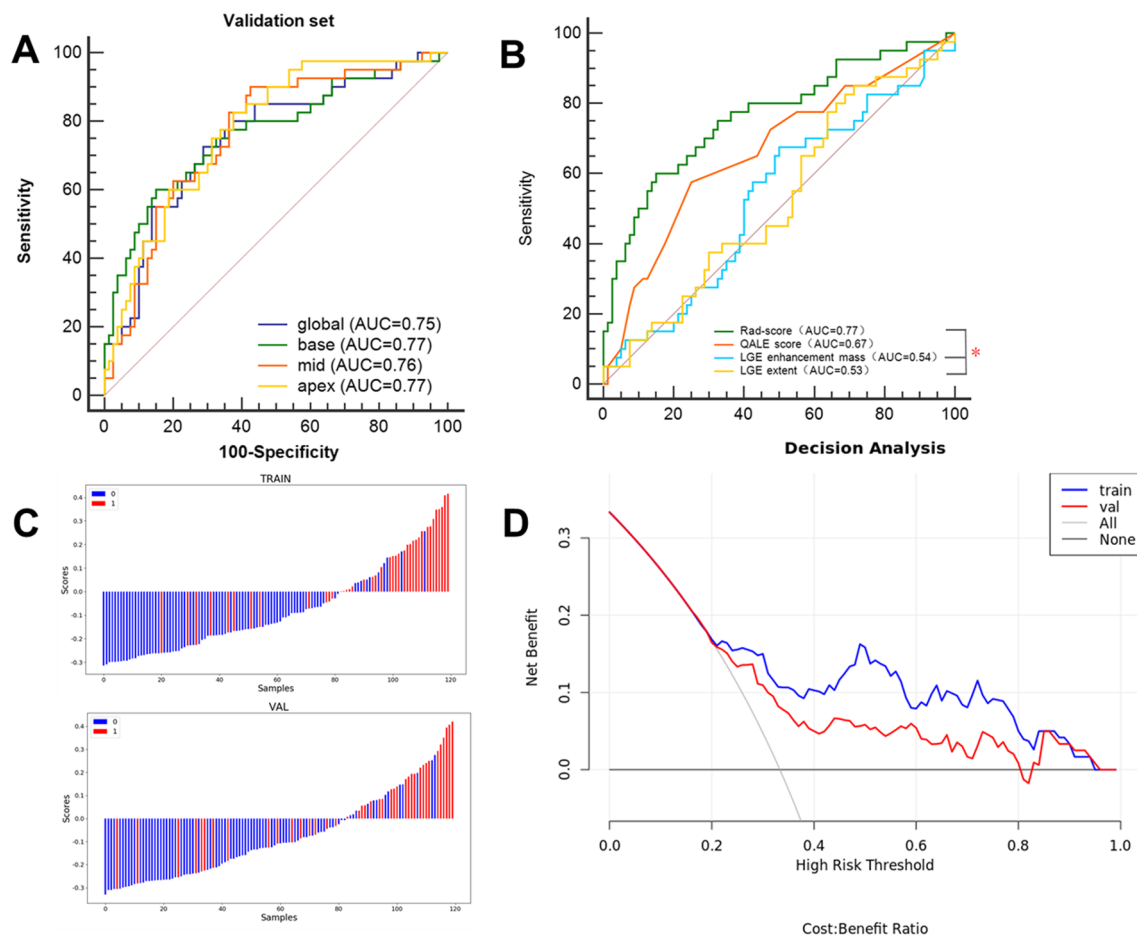

Fig. 2 ROC curve analysis for radiomics model of different sections in the validation set (**A**); ROC curves analysis for comparison of predictive performance of LV base-radiomics with semi-quantitative and quantitative LGE parameters (**B**); Rad-score for each patient in the training and validation sets (**C**); decision curve for the radiomics model in the training and validation sets (**D**)

wavelet-based, two Laplacian of Gaussian–based, and three logarithm-based features (Supplemental Fig. 1).

Predictive performance and clinical utility of radiomics models

Table 2 shows the predictive performance of the radiomics model for different sections. In the validation set, the AUC was 0.75, 0.77, 0.76, and 0.77 in the global LV, base, mid-ventricle, and apex, respectively (Fig. 2A). The DeLong test showed no statistical difference in AUC between different sections (all $p > 0.05$). Basal radiomics model was selected for further prognostic analysis.

The AUC of the basal Rad-score was higher than that of LGE total enhancement mass (0.77 vs. 0.54, $p < 0.001$) and LGE extent (0.77 vs. 0.53, $p = 0.004$) (Fig. 2B). Supplemental Table 2 shows the predictive performance of cardiac functional and LGE semi-quantitative and quantitative parameters in detail. The basal Rad-score of each patient in the training and validation sets is shown in Fig. 2C, which further confirms that radiomics can predict the adverse event of CA.

To estimate the clinical utility of established models, decision curve analysis (DCA) was performed by quantifying the net benefits at different threshold probabilities in the validation dataset and showed that both the training and validation sets to predict all-cause mortality had more benefit than either the "treat-all" model or the "treat-none" model (Fig. 2D).

Survival analysis and risk stratification

During a median follow-up duration of 12.9 months, a total of 40 CA patients died. Univariate survival analysis showed sex, age, diabetes, Mayo stage, QALE, LVEF, LVEDV, LVESV, and Rad-score were considered as factors for risk stratification of all-cause mortality in CA. ROC curves of the six factors with higher AUC are shown in Fig. 3A. Although the AUC of Mayo stage was higher than Rad-score, there was no

statistically significant difference (0.81 vs. 0.77, $p = 0.40$). We further evaluated the predictive performance of Rad-score combined with Mayo stage and found that the AUC of their combination was higher than that of Mayo stage alone (0.86 vs. 0.81, $p = 0.03$) or Rad-score alone (0.86 vs. 0.77, $p = 0.01$), as shown in Fig. 3B. Other imaging indices such as EF, LGE semi-quantitative, and quantitative parameters combined with Mayo stage had no incremental value.

Survival of patients was stratified by the risk classification according to the Rad-score cut-off value of 0.66, which was the best predictor of survival (HR 8.91; 95% CI, 3.89–20.44; $p < 0.001$) (Fig. 4). The survival curve indicates that there is an approximately 84% chance of survival at 12 months in patients with the Rad-score < 0.66 compared with 33% for patients with Rad-score ≥ 0.66. Figure 5 shows the radiomics analysis and prognosis correlation from LGE images of three CA patients, which suggests that radiomics model is a better prognostic assessment for CA.

Discussion

To the best of our knowledge, this is the first study focusing on the prognostic value of radiomics analysis based on LGE images in CA. The results of this study suggest that LGE-based radiomics features are associated with all-cause mortality in CA patients, which can be a helpful risk stratification tool in CA patients. The main findings of this study include the following: (1) The predictive performance of the radiomics model was similar in different sections of LV in the validation set, and the predictive performance of the basal radiomics model was superior to the LGE semi-quantitative and quantitative parameters; (2) Rad-score combined with Mayo stage further improved the predictive performance of adverse events in CA, suggesting that radiomics features have incremental value for clinical stage; (3) Rad-score ≥ 0.66 was associated with a significantly increased risk of all-cause mortality in CA patients.

Fig. 3 ROC curve of single factor (**A**) and Rad-score combined with Mayo stage (**B**). Graphs show AUC of the Rad-score combined with Mayo stage is higher than those of the Mayo stage alone and the Rad-score alone. Asterisk represents a statistical difference
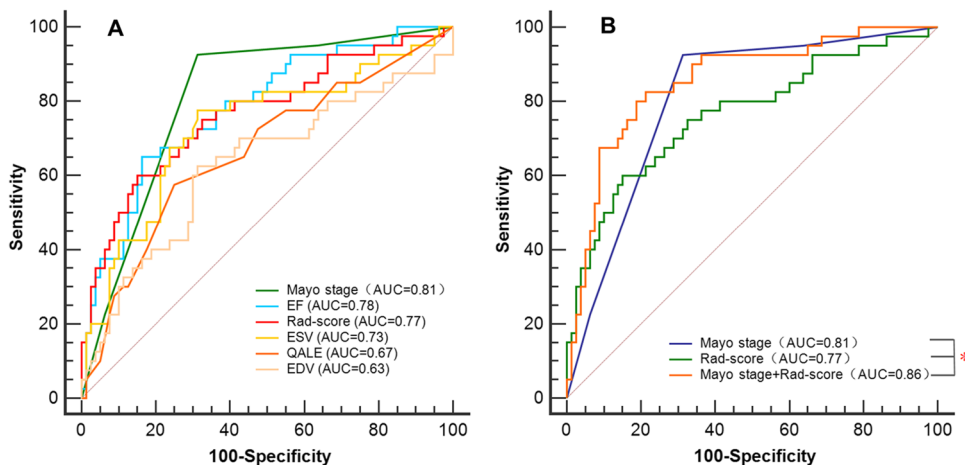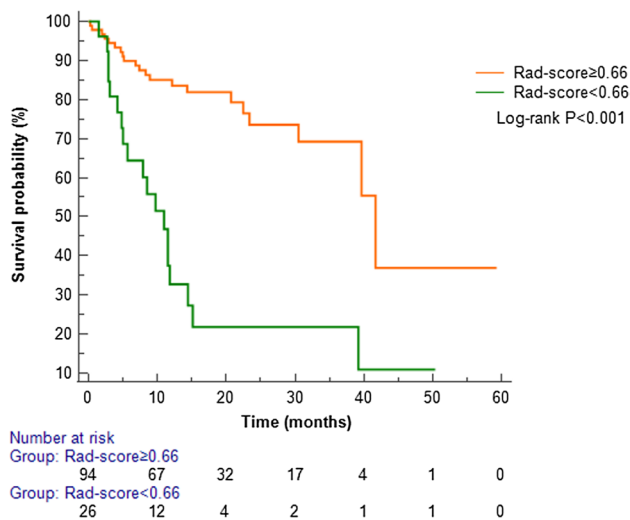
Fig. 4 Kaplan–Meier survival curves of Rad-score. Survival probability differs significantly categorized by Rad-score cut-off values of 0.66

The development of CMR technology has proposed numerous new imaging biomarkers for CA prognosis. Transmural LGE, T1 elevation, and extracellular volume all correlate with amyloid load and provide incremental information of clinical outcome [12, 14, 27]. For example, Kotecha et al [28] found that the T2 value was a predictor of prognosis in AL amyloidosis. Some new CMR techniques, such as CMR tagging, are considered essential to measure regional myocardial function and contribute to the quantitative assessment of local myocardial motion and strain, thus reflecting

the severity of cardiac amyloid deposition [29, 30]. However, these indicators of CA on CMR imaging including the presence of LGE and more quantitative parameters do not reflect the microscopic information of the disease and may overlook some important prognostic information. Developments in radiomics have changed the way of interpreting images, thereby potentially improving diagnostic, prognostic, and predictive accuracy. A study by Kotu et al [20] demonstrated that texture features extracted from LGE images improved arrhythmic risk stratification in post-myocardial infarction patients. Amano et al [31] found that texture analysis may provide information about LGE related to ventricular tachyarrhythmias in hypertrophic cardiomyopathy. Our study confirmed the association of radiomics features with all-cause mortality in CA patients using LGE images, highlighting the value of radiomics in the prognosis of cardiovascular disease.

The Mayo staging system is an important clinical tool for risk stratification in patients with AL amyloidosis [9]. Our previous study [32] demonstrated that radiomics features were moderately correlated with Mayo stage, suggesting that radiomics features may reflect prognosis of CA. This study confirmed that the risk of death was significantly increased when Rad-score ≥ 0.66. Therefore, Rad-score can be a new imaging indicator for CA risk stratification. Moreover, radiomics features can provide incremental value relative to clinical prognostic predictors.

Our previous research demonstrated no significant differences in the diagnostic performance of radiomics models for different sections of the LV [32]. In this study, radiomics models were still constructed based on these sections, and we further found that their predictive performance differed in the

Fig. 5 Representative LGE images of CA patients. Panel **A** Base, mid, and apex—LV short-axis LGE MR images depict a focal, patchy LGE pattern in a 62-year-old woman with CA. This patient had no adverse events during 3 years follow-up. Panel **B** A 36-year-old male patient had transmural LGE at the base and subendocardial LGE in the middle and apical sections of LV. This patient died suddenly after 1 year of follow-up. Panel **C** A 59-year-old man had a low LGE extent but a high Rad-score of 0.83 (> 0.66), who died of cardiac arrest during 1 year of follow-up
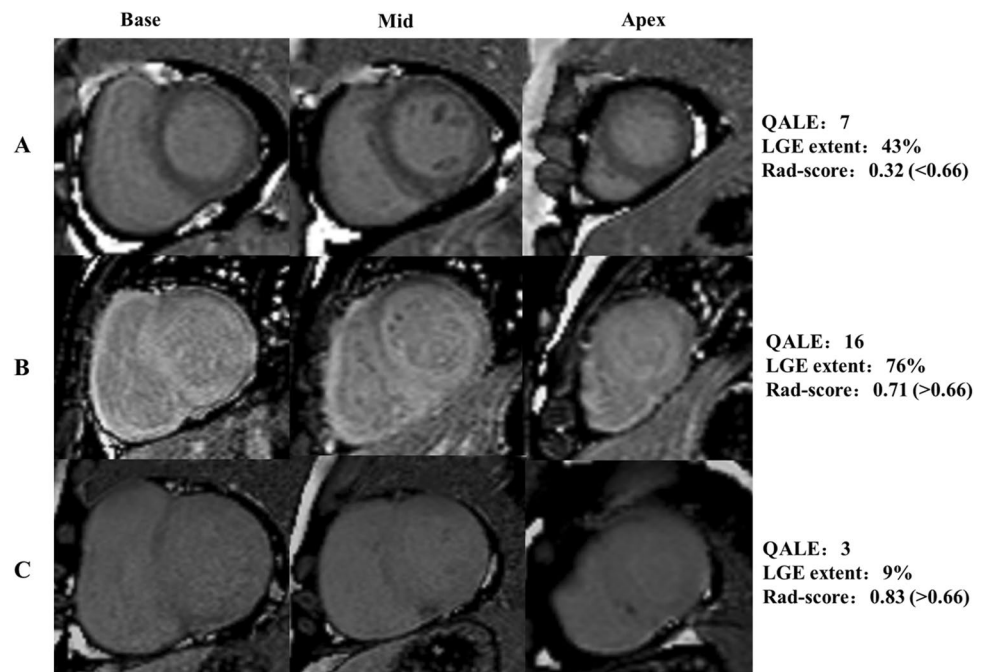
training set, but did not show statistically significant differences in the validation set. This was similar to the results of our previous study [32], indicating that there was no significant difference in the diagnosis and prognosis of CA between radiomics features extracted from different sections, further confirming the rationality of selecting only base-LV for analysis. This finding did not seem to support the regional variation of LGE distribution in patients with CA. It is speculated that although amyloid load shows a significant base-to-apex gradient, all myocardium has already undergone at least subtle pathological changes, which can be easily detected by radiomics.

LGE-CMR is a classic imaging tool to analyze CA. However, accurate quantification of amyloid infiltration on LGE is challenging, because CA is typically a diffuse disease with mixing of the normal and the diseased myocardium. Therefore, the true severity of the lesion can be underestimated in patients with mild or diffuse lesions. Patients in the event-positive and event-negative groups in this study did not show statistically significant differences in quantitative LGE parameters. This may be because patients in the positive group had more severe myocardial involvement, making it difficult to outline the normal myocardial regions, and thus the quantitative LGE measurements were underestimated. The underlying mechanism remains to deserve further study.

Radiomics analysis is of clinical importance in CA. The radiomics score is expected to be incorporated into the Mayo staging system to create a new staging system and will help develop risk-adapted therapies for AL amyloidosis. Radiomics score combined with Mayo stage allows better classification of patients and helps to develop and test treatment strategies for specific patient groups in terms of clinical outcome.

There are several limitations in this preliminary study. First, it was a retrospective study and potential bias was not avoided; for example, we did not include ATTR form of the disease in this study. Second, the sample size of study subjects was limited and the follow-up duration was short with inconsistent time of follow-up endpoints across three centers. Third, no patients had undergone endomyocardial biopsy, thus lacking pathological evidence of myocardial involvement. Fourth, only all-cause mortality was used as primary outcome, data regarding cardiovascular outcomes were not available. Fifth, the population of this study was entirely composed of patients with AL CA, so the prognosis of radiomics in patients with different subtypes of CA still requires further studies. Sixth, different MRI parameters were used in this study. Finally, this study was only based on LGE images for radiomics analysis, and future studies on radiomics from other sequences such as T1 or T2 mapping are needed.

In conclusion, this study shows radiomics has better predictive performance than LGE semi-quantitative and quantitative parameters for poor prognosis in CA and may provide incremental value and improve risk stratification for all-cause mortality in patients with AL amyloidosis.

Declarations

Guarantor The scientific guarantor of this publication is Long Jiang Zhang, Department of Radiology, Jinling Hospital, Medical School of Nanjing University, Nanjing 210002, Jiangsu, China.

Conflict of interest The authors of this manuscript declare no relationships with any companies whose products or services may be related to the subject matter of the article.

Statistics and biometry No complex statistical methods were necessary for this paper.

Informed consent Written informed consent was waived by the institutional review board.

Ethical approval Institutional review board approval was obtained.

Study subjects or cohorts overlap Our previous research included 200 patients with AL amyloidosis, including 139 internal data and 61 external data to assess the potential of a radiomics approach of LGE-CMR in the diagnosis of CA, and found that radiomics approach is a useful and complementary tool for the detection of CA. In this multicenter study, we included 120 patients with cardiac involvement among these 200 patients with AL amyloidosis to evaluate the prognostic value of radiomics.

Some study subjects or cohorts have been previously reported in a study. (Zhou XY, Tang CX, Guo YK et al (2022) Diagnosis of cardiac amyloidosis using a radiomics approach applied to late gadolinium-enhanced cardiac magnetic resonance images: a retrospective, multicohort, diagnostic study. *Frontiers in Cardiovascular Medicine* 9:818957).

Methodology
● Retrospective
● Prognostic study
● Multicenter study

References

1. Ridouani F, Damy T, Tacher V et al (2018) Myocardial native T2 measurement to differentiate light-chain and transthyretin cardiac amyloidosis and assess prognosis. J Cardiovasc Magn Reson 20:58
2. Falk RH, Alexander KM, Liao R, Dorbala S (2016) AL (Light-Chain) Cardiac amyloidosis: a review of diagnosis and therapy. J Am Coll Cardiol 68:1323–1341
3. Rubin J, Maurer MS (2020) Cardiac amyloidosis: overlooked, underappreciated, and treatable. Annu Rev Med 71:203–219
4. Gertz MA, Dispenzieri A, Sher T (2015) Pathophysiology and treatment of cardiac amyloidosis. Nat Rev Cardiol 12:91–102
5. Arenja N, Andre F, Riffel JH et al (2019) Prognostic value of novel imaging parameters derived from standard cardiovascular magnetic resonance in high risk patients with systemic light chain amyloidosis. J Cardiovasc Magn Reson 21:53
6. Banypersad SM, Fontana M, Maestrini V et al (2015) T1 mapping and survival in systemic light-chain amyloidosis. Eur Heart J 36:244–251

7. Fontana M, Corovic A, Scully P, Moon JC (2019) Myocardial amyloidosis: the exemplar interstitial disease. JACC Cardiovasc Imaging 12:2345–2356

8. Dorbala S, Cuddy S, Falk RH (2020) How to image cardiac amyloidosis: a practical approach. JACC Cardiovasc Imaging 13:1368–1383

9. Kumar S, Dispenzieri A, Lacy MQ et al (2012) Revised prognostic staging system for light chain amyloidosis incorporating cardiac biomarkers and serum free light chain measurements. J Clin Oncol 30:989–995

10. Pregenzer-Wenzler A, Abraham J, Barrell K, Kovacsovics T, Nativi-Nicolau J (2020) Utility of biomarkers in cardiac amyloidosis. JACC Heart Fail 8:701–711

11. Fontana M, Chung R, Hawkins PN, Moon JC (2015) Cardiovascular magnetic resonance for amyloidosis. Heart Fail Rev 20:133–144

12. Fontana M, Pica S, Reant P et al (2015) Prognostic value of late gadolinium enhancement cardiovascular magnetic resonance in cardiac amyloidosis. Circulation 132:1570–1579

13. Wan K, Li W, Sun J et al (2019) Regional amyloid distribution and impact on mortality in light-chain amyloidosis: a T1 mapping cardiac magnetic resonance study. Amyloid 26:45–51

14. Raina S, Lensing SY, Nairooz RS et al (2016) Prognostic value of late gadolinium enhancement CMR in systemic amyloidosis. JACC Cardiovasc Imaging 9:1267–1277

15. Raisi-Estabragh Z, Izquierdo C, Campello VM et al (2020) Cardiac magnetic resonance radiomics: basic principles and clinical perspectives. Eur Heart J Cardiovasc Imaging 21:349–356

16. Avanzo M, Stancanello J, El Naqa I (2017) Beyond imaging: the promise of radiomics. Phys Med 38:122–139

17. Gillies RJ, Kinahan PE, Hricak H (2016) Radiomics: images are more than pictures, they are data. Radiology 278:563–577

18. Cheng S, Fang M, Cui C et al (2018) LGE-CMR-derived texture features reflect poor prognosis in hypertrophic cardiomyopathy patients with systolic dysfunction: preliminary results. Eur Radiol 28:4615–4624

19. Ma Q, Ma Y, Wang X et al (2021) A radiomic nomogram for prediction of major adverse cardiac events in ST-segment elevation myocardial infarction. Eur Radiol 31:1140–1150

20. Kotu LP, Engan K, Borhani R et al (2015) Cardiac magnetic resonance image-based classification of the risk of arrhythmias in post-myocardial infarction patients. Artif Intell Med 64:205–215

21. Ma Q, Ma Y, Yu T, Sun Z, Hou Y (2021) Radiomics of non-contrast-enhanced T1 mapping: diagnostic and predictive performance for myocardial injury in acute ST-segment-elevation myocardial infarction. Korean J Radiol 22:535–546

22. Dorbala S, Ando Y, Bokhari S et al (2020) ASNC/AHA/ASE/EANM/HFSA/ISA/SCMR/SNMMI expert consensus recommendations for multimodality imaging in cardiac amyloidosis: Part 2 of 2-Diagnostic criteria and appropriate utilization. J Nucl Cardiol 27:659–673

23. Garcia-Pavia P, Rapezzi C, Adler Y et al (2021) Diagnosis and treatment of cardiac amyloidosis: a position statement of the ESC Working Group on Myocardial and Pericardial Diseases. Eur Heart J 42:1554–1568

24. Dungu JN, Valencia O, Pinney JH et al (2014) CMR-based differentiation of AL and ATTR cardiac amyloidosis. JACC Cardiovasc Imaging 7:133–142

25. Wan K, Sun J, Han Y et al (2018) Increased prognostic value of query amyloid late enhancement score in light-chain cardiac amyloidosis. Circ J 82:739–746

26. Williams LK, Forero JF, Popovic ZB et al (2017) Patterns of CMR measured longitudinal strain and its association with late gadolinium enhancement in patients with cardiac amyloidosis and its mimics. J Cardiovasc Magn Reson 19:61

27. Boynton SJ, Geske JB, Dispenzieri A et al (2016) LGE provides incremental prognostic information over serum biomarkers in AL cardiac amyloidosis. JACC Cardiovasc Imaging 9:680–686

28. Kotecha T, Martinez-Naharro A, Treibel TA et al (2018) Myocardial edema and prognosis in amyloidosis. J Am Coll Cardiol 71:2919–2931

29 Jeung MY, Germain P, Croisille P, El ghannudi S, Roy C, Gangi A (2012) Myocardial tagging with MR imaging: overview of normal and pathologic findings. Radiographics 32:1381–1398

30. Oda S, Utsunomiya D, Nakaura T et al (2017) Identification and assessment of cardiac amyloidosis by myocardial strain analysis of cardiac magnetic resonance imaging. Circ J 81:1014–1021

31. Amano Y, Suzuki Y, Yanagisawa F, Omori Y, Matsumoto N (2018) Relationship between extension or texture features of late gadolinium enhancement and ventricular tachyarrhythmias in hypertrophic cardiomyopathy. Biomed Res Int 2018:4092469

32. Zhou XY, Tang CX, Guo YK et al (2022) Diagnosis of cardiac amyloidosis using a radiomics approach applied to late gadolinium-enhanced cardiac magnetic resonance images: a retrospective, multicohort, diagnostic study. Front Cardiovasc Med 9:818957